

~~CONFIDENTIAL~~

UNCLASSIFIED



RESEARCH MEMORANDUM

INVESTIGATION OF THE DISTRIBUTION OF LIFT,
DRAG, AND PITCHING MOMENT BETWEEN THE WING AND FUSELAGE OF
A $\frac{1}{30}$ - SCALE SEMISPAN MODEL OF THE BELL X-5 AIRPLANE AT A
MACH NUMBER OF 1.24 BY THE NACA WING-FLOW METHOD

By Norman S. Silsby and Garland J. Morris

Langley Aeronautical Laboratory
Langley Field, Va.

CLASSIFICATION CANCELLED

FOR REFERENCE

Authority NACA R 7 2824 Date 10/29/54

By mxg 11/24/54 See _____

NOT TO BE TAKEN FROM THIS ROOM

CLASSIFIED DOCUMENT

This material contains information affecting the National Defense of the United States within the meaning of the espionage laws, Title 18, U.S.C., Secs. 793 and 794, the transmission or revelation of which in any manner to unauthorized person is prohibited by law.

NATIONAL ADVISORY COMMITTEE FOR AERONAUTICS

WASHINGTON

January 16, 1952

UNCLASSIFIED

~~CONFIDENTIAL~~

NACA RM L51K27



UNCLASSIFIED

NATIONAL ADVISORY COMMITTEE FOR AERONAUTICS

RESEARCH MEMORANDUM

INVESTIGATION OF THE DISTRIBUTION OF LIFT,
 DRAG, AND PITCHING MOMENT BETWEEN THE WING AND FUSELAGE OF
 A $\frac{1}{30}$ - SCALE SEMISPAN MODEL OF THE BELL X-5 AIRPLANE AT A
 MACH NUMBER OF 1.24 BY THE NACA WING-FLOW METHOD

By Norman S. Silsby and Garland J. Morris

SUMMARY

An investigation has been made at a Mach number of 1.24 by the NACA wing-flow method to determine the distribution of lift, drag, and pitching moment between the wing and fuselage of a $\frac{1}{30}$ - scale semispan model of the Bell X-5 airplane. Lift, drag, pitching moments, and wing bending moments were obtained for various angles of attack for 40° , 50° , and 60° sweptback duralumin wings in the presence of, but detached from, the fuselage. In addition, tests were also made of a 60° sweptback wooden wing in combination with the fuselage both with and without a horizontal tail to determine the effect of wing flexibility on the longitudinal stability characteristics. Results of the present tests are compared with previous tests. The Reynolds number of the tests was about 1.0×10^6 .

For all sweep angles tested, the proportion of total lift carried over on the fuselage was approximately equal to the ratio of the area between the wing-fuselage intersections to the total wing area. The lateral center-of-pressure location for the exposed wing moved outboard from 43 percent span of the exposed wing for 40° sweep to 50 percent of the exposed wing for 60° sweep.

The wing interference on the fuselage tended to create a stabilizing effect, particularly at small angles of attack, which, at least partially offsets the destabilizing contribution of the isolated fuselage.

The effect of increasing the flexibility of the 60° wing in bending by about $2\frac{1}{2}$ times was to reduce the lift-curve slope about 3 percent and to move the aerodynamic center forward about 4 percent of the mean aerodynamic chord.

UNCLASSIFIED

INTRODUCTION

As part of a program to determine the aerodynamic characteristics of the Bell X-5 airplane incorporating a wing whose angle of sweep can be varied in flight, an investigation was made at low supersonic speeds by the NACA wing-flow method on a $\frac{1}{30}$ -scale semispan model. Results of tests to determine the longitudinal stability characteristics of this model with the wing sweptback 60° , the effect of sweepback on the longitudinal stability characteristics, the longitudinal-control effectiveness and downwash characteristics, and the effects of fuselage flap-type dive brakes on the aerodynamic characteristics have been reported in references 1 to 4, respectively.

This paper presents results of tests made to determine the distribution of lift, drag, and pitching moment between the fuselage and wings sweptback 40° , 50° , and 60° . In addition, the root bending moments of these wings and the effect of wing flexibility on the longitudinal stability characteristics of the model with the wing sweptback 60° were determined. This paper presents results of measurements of normal force, chord force, pitching moment and wing bending moment for the various configurations over a range of angles of attack. The effective Mach number at the wing of the model for the tests was about 1.24 and the Reynolds number was of the order of 1.0×10^6 .

SYMBOLS

- B bending moment of exposed wing about wing pivot point, inch-pounds
- $b/2$ model wing span, inches
- $b_1/2$ distance from pivot point to model wing tip, inches
- c local wing chord parallel to plane of symmetry (position of wing within fuselage is considered to be formed by perpendiculars from wing-fuselage intersection to plane of symmetry), inches
- \bar{c} mean aerodynamic chord of wing based on the relationship

$$\frac{\int_0^{b/2} c^2 dy}{\int_0^{b/2} c dy}, \text{ inches}$$

\bar{c}_t	mean aerodynamic chord of tail, inches
C_B	bending-moment coefficient about wing pivot point $\left(\frac{B}{qS_e \frac{b_1}{2}} \right)$
C_D	drag coefficient (D/qS)
C_{DF}	drag coefficient of fuselage (based on wing area)
C_L	lift coefficient (L/qS)
C_m	pitching-moment coefficient $(M/qS\bar{c})$
C_N	normal-force coefficient, based on exposed wing area
$C_{L\alpha}$	rate of change of lift coefficient with angle of attack
$C_{m\alpha}$	rate of change of pitching-moment coefficient with angle of attack referred to $0.26\bar{c}$
D	drag, pounds
i_t	incidence of horizontal tail (referred to wing-chord plane), degrees
L	lift, pounds
M	pitching moment about center line of balance, inch-pounds
M_L	local Mach number at wing surface of North American F-51D airplane
M_t	effective Mach number for tail of model
M_w	effective Mach number for wing of model
q	effective dynamic pressure for the wing of the model, pounds per square foot $\left(\frac{1}{2} \rho V^2 \right)$
R	Reynolds number based on mean aerodynamic chord \bar{c}
S	wing area, semispan model, square feet $\left(\int_0^{b/2} c \, dy \right)$

S_e	exposed wing area, semispan model, square feet
V	velocity, feet per second
y	spanwise coordinate, inches
\bar{y}	lateral center-of-pressure location (from pivot point), inches $\left(\frac{C_B b_1}{C_N 2} \right)$
α	angle of attack (referred to wing-chord plane), degrees
Λ	sweepback angle referred to 25-percent chord line of 50° wing
ρ	mass density, slugs per cubic foot

A prime indicates coefficients based on dimensions of configuration with 60° sweptback wing.

A subscript 0 refers to zero lift.

APPARATUS AND TESTS

The tests were made by the NACA wing-flow method in which the model is mounted in a region of high-speed flow over the wing of a North American F-51D airplane. The contour of the airplane wing in the test region for the present investigation was designed to give a uniform velocity field at Mach numbers near 1.25 at a flight Mach number of approximately 0.71.

The components of the semispan model of the Bell X-5 airplane consisted of three dural wings sweptback 40°, 50°, and 60°, one wood wing with a steel core sweptback 60°, a fuselage equipped with an end plate, and a horizontal tail of -6° incidence. Except for the wood wing, which had the same dimensions as the 60° sweptback dural wing, these components were the same as those used in references 1 to 3. Some of the geometric characteristics of the model are given in figures 1 and 2 and table 1.

In tests to determine the distribution of lift between the wing and fuselage the dural wings were separated from the fuselage by a suitable gap to allow for the measurement of forces on the wing in the presence of the fuselage (see fig. 3). A small end plate was attached to the wings near the wing-fuselage juncture and was spaced from the fuselage by about 0.02 inch to minimize the leakage of air through the gap between the wing and fuselage (figs. 3 and 4). These configurations

were tested without the horizontal tail. The wing shank, which passed through the skin of the F-51D wing, was equipped with strain gages to measure the bending moments of the wing of the model in presence of the fuselage.

In a test made to determine the effect of the gap used between the wing and fuselage in the wing-detached tests the wing was attached to the fuselage, and the gap in the fuselage around the wing was approximately simulated.

The 60° sweptback wood wing was tested in combination with the fuselage without the horizontal tail and with the tail having an incidence of -6° (fig. 5) in order to indicate the effect of flexibility on the aerodynamic characteristics. The wing was built of laminated birch wood with a small steel core (fig. 2). Static load tests indicated that the wood wing was about 42 percent as stiff, in bending, as the dural wing.

In order to facilitate reference to the various test configurations the following abbreviated designations have been adopted:

Wing-Detached Configurations

<u>Designation</u>	<u>Description of configuration</u>
$W_{Ad}^F eg$	40°, 50°, and 60° sweptback dural wings in the presence of but detached d from the fuselage, with a small end plate e attached to the root of the wing with a gap g of about 0.02 inch from the fuselage; no horizontal tail
$W_{40d}^F eg$	
$W_{50d}^F eg$	
$W_{60d}^F eg$	

Wing-Attached Configurations

W_{Λ}^F	dural wing-fuselage configuration of reference 3
$W_{60}^F eg$	60° dural wing-fuselage configuration with wing end plate e; gap g around fuselage of configurations $W_{Ad}^F eg$ approximately simulated; no horizontal tail
W_{w60}^F	60° wood w wing-fuselage configuration; no horizontal tail
W_{w60}^{FT-6}	60° wood w wing-fuselage configuration with horizontal tail; $i_t = -6^\circ$

W_{60}^{FT-6} 60° dural wing-fuselage configuration with horizontal tail; $i_t = -6^\circ$ (reference 1)

Other Configurations

F fuselage alone configuration of reference 2

$W_{\Delta F} - F$ results obtained by combining data of configuration $W_{\Delta F}$ and configuration F as described in text

The model was originally designed and constructed so that the pitching moment would be measured about the 25-percent mean-aerodynamic-chord position (gross weight center of gravity of the full-scale airplane) of the wing in each sweep position. However, subsequent changes in wing span and fillets resulted in the fact that the position about which the pitching moments were measured corresponded to the 35-, 29-, and 26-percent mean aerodynamic chord of the 40°, 50°, and 60° wings, respectively.

A typical chordwise Mach number distribution in the test region on the airplane wing as determined from static pressure measurements at the wing surface with the model removed is indicated in figure 6. The method of determining the effective dynamic pressure at the model wing q and the effective Mach number at the model wing M_w can be found in references 1 and 5.

The method of testing was similar to that described in references 1 to 3. For the present tests, the Mach number of the wing of the model was about 1.24. The Reynolds number was about $0.9 \times 10^6 \pm 9$ percent for the 40° wing, $0.9 \times 10^6 \pm 3$ percent for the 50° wing, and $1.1 \times 10^6 \pm 9$ percent for the 60° wing based on their respective mean aerodynamic chords.

PRESENTATION OF RESULTS

The results are presented in figures 7 to 15. The following table lists the quantities and configurations shown and the figure numbers in which they appear:

Quantity	Configurations	Figure number
C_L and C_m against α ; C_L against C_D	W_{40d}^{Feg} W_{50d}^{Feg}	7(a) 7(b)
C_L' and C_m' against α ; C_L' against C_D'	W_{60d}^{Feg} W_{60}^{Feg}	7(c) 8
C_B against C_N	W_{Ad}^{Feg}	9
C_L and C_L' against α	W_{Ad}^{Feg} ; W_{60}^{Feg} ; W_{Λ}^F	10
C_D and C_D' against α	W_{Ad}^{Feg} ; W_{Λ}^F ; W_{60}^{Feg} ; $W_{\Lambda}^F - F$; $W_{60}^{Feg} - F$; F	11
C_m and C_m' against α	W_{Ad}^{Feg} ; W_{60}^{Feg} ; W_{Λ}^F ; F	12
$\frac{\bar{y}}{b_1/2}$, C_D' , $C_{L\alpha}'$, and $C_{m\alpha}'$ against Λ	W_{Ad}^{Feg} ; W_{Λ}^F ; W_{60}^{Feg} ; F ; $W_{\Lambda}^F - F$; $W_{60}^{Feg} - F$; $W_{\Lambda}^F - W_{Ad}^{Feg}$	13
C_L' and C_m' against α ; C_L' against C_D'	W_{w60}^{FT-6} W_{w60}^F W_{60}^{FT-6} ; W_{w60}^{FT-6} W_{60}^F ; W_{w60}^F	14(a) 14(b) 15(a) 15(b)

The calculated variation of C_D with α (fig. 11) for the exposed wing (configuration $W_{\Lambda}^F - F$) was obtained from the expression

$$C_{D_{W_{\Lambda}^F - F}} = C_{D_{(W_{\Lambda}^F)_0}} - C_{D_F} + \left(C_{D_{W_{\Lambda}^F}} - C_{D_{(W_{\Lambda}^F)_0}} \right) \frac{S_e}{S} \quad (1)$$

where the final term takes into account the induced drag of the exposed wing. A similar expression was used to determine C_D for configuration

$W_{60}^{F_{eg}} - F$. The values of C_D' for configuration $W_{Ad}^{F_{eg}}$ and the values of C_D' for configuration F (fig. 13) which were used in the computation of values of C_D' for configurations $W_{AF} - F$ and $W_{60}^{F_{eg}} - F$ were obtained at the same angles of attack as for the W_{AF} configuration at lift coefficients C_L' of 0 and 0.4. Similarly, the values of $C_{m\alpha}'$ (fig. 13) for configuration $W_{Ad}^{F_{eg}}$ were obtained at the same angles of attack as for configuration W_{AF} at lift coefficients C_L' of 0 and 0.4.

DISCUSSION

Lift Characteristics

A comparison of the variation of lift coefficient with angle of attack for configurations W_{60}^F and $W_{60}^{F_{eg}}$ (fig. 10) shows the same lift-curve slope, indicating no effect of the gap on the lift characteristics.

The lift-curve slopes over the linear portion of the curves for configurations $W_{40d}^{F_{eg}}$, $W_{50d}^{F_{eg}}$, and $W_{60d}^{F_{eg}}$ are 0.049, 0.049, and 0.039, respectively. These compare with values of lift-curve slope for the W_{AF} configurations (reference 3) of 0.063, 0.062, and 0.052 for the 40° , 50° , and 60° wings, respectively. It will be noted that in both cases there is little or no change in lift-curve slope between 40° and 50° sweep. This result is substantiated by a number of other tests with a tail on (see reference 3). If the values of lift-curve slopes of configurations $W_{40d}^{F_{eg}}$, $W_{50d}^{F_{eg}}$, and $W_{60d}^{F_{eg}}$ (fig. 10) are adjusted, respectively, by the ratios of the total wing area (which includes that portion in the fuselage between perpendiculars from wing-fuselage intersections to the plane of symmetry), to the exposed wing area (1.295, 1.31, 1.31), the resulting values of lift-curve slope are 0.0635, 0.064, and 0.051, which are very nearly equal to the values for configurations W_{AF} . Thus the proportion of total lift carried over on the fuselage is about equal to the ratio of areas between the fuselage-wing intersection to the total wing area. The lift-curve slopes $C_{L\alpha}'$ for configurations W_{AF} and $W_{Ad}^{F_{eg}}$ (fig. 13) decrease with increasing sweepback angle, and at 60° sweep, the slopes are about 74 percent of the values at 40° sweep. The decrease in $C_{L\alpha}'$ between sweep angles of 40° and 50° is due to the decrease in wing area as the sweep angle is increased. The fuselage

contributes a constant increment in $C_{L\alpha}$ of 0.012 (based on the 60° wing area) for the three sweepback angles tested.

The lateral center-of-pressure location for configuration W_{Ad}^{Feg} (fig. 13) moved outboard of the pivot point from 43 percent of the span of the exposed wing for 40° of sweepback to about 50 percent of the exposed wing span for 60° of sweepback.

Drag Characteristics

A comparison of the drag coefficients of the W_{60d}^{Feg} and $W_{60}^{Feg} - F$ configurations (fig. 11) indicate that, over a range of angles of attack of -2° to 12° , configuration $W_{60}^{Feg} - F$ has a small favorable interference effect on the drag of the fuselage of 10 to 15 percent of the wing drag. The interference of the wing in the W_{60}^{Feg} configuration on the drag of the fuselage is therefore believed to be of the same order. A similar comparison for the 50° and 40° sweepback cases cannot be made since no results are available for the W_{50}^{Feg} and W_{40}^{Feg} configurations. Because of the appreciable effect of the end plate and gap on drag as may be noted for configurations $W_{60}^{Feg} - F$ and $W_{60}^{Feg} - F$ (fig. 11), the difference in values of C_D for W_{Ad}^{Feg} and $W_{\Lambda}^{Feg} - F$ configurations do not indicate the interference effect of the wing on the fuselage (fig. 13). For the same reason the absolute values of drag coefficient of configurations W_{Ad}^{Feg} are not considered to be reliable.

Pitching-Moment Characteristics

A comparison of the variation of pitching-moment coefficient with angle of attack for configurations W_{60}^{Feg} and W_{60}^{Feg} (fig. 12) indicates that the gap and end plate at the wing-fuselage junction of the W_{60}^{Feg} configuration has little effect on the zero-lift moment but does have some destabilizing effect equivalent to a forward shift in aerodynamic center averaging about 2.5 percent \bar{c} over the range of angles of attack covered. Whether this effect arises from changes in flow over the fuselage or over the wing was not determined and therefore the contributions of the wing interference on the fuselage to the stability as indicated by comparisons of the pitching-moment data for configurations W_{Ad}^{Feg} , W_{Λ}^{Feg} , and F should be considered as qualitative.

The fuselage in the presence of the wing (see fig. 12) gives a nose-down pitching moment at $\alpha = 0^\circ$ or $C_L = 0$ which is somewhat greater (15 to 30 percent depending on sweep angle) than that for the isolated fuselage (reference 2).

A comparison of the stability parameter $C_{m\alpha}'$ for configurations $W_{\Delta d}^F eg$ and W_{Δ}^F (fig. 13) shows that at low lift coefficients there is little or no difference, indicating that the lift load carried over on the fuselage from the wing has a stabilizing effect which largely offsets the unstable moment variation of the fuselage itself. At the higher lift coefficients (about 0.4) the fuselage in the presence of the wing does reduce the stability but the amount of the change is still less than the unstable $C_{m\alpha}'$ of the isolated fuselage. The $C_{m\alpha}'$ for the fuselage as determined from $W_{\Delta}^F - W_{\Delta d}^F eg$ indicates a stabilizing effect of wing interference on the fuselage as compared to $C_{m\alpha}'$ for the isolated fuselage.

A comparison of the values of $C_{m\alpha}'$ for the $W_{60}^F eg$ and $W_{60d}^F eg$ configurations where the gap and end plate effects are present in both cases suggests that the stabilizing effect of the wing interference on the fuselage may be somewhat less than is indicated by the comparisons of W_{Δ}^F and $W_{\Delta d}^F eg$.

Flexibility

Substitution of the wooden wing (about 42 percent as rigid in bending as the dural wing) resulted in a 4-percent decrease in lift-curve slope for configuration W_{w60}^{FT-6} (fig. 15(a)) and a 2 percent decrease for the W_{w60}^F configuration (fig. 15(b)). This reduction in lift-curve slope is in agreement with the fact that bending of a swept-back wing effectively reduces the local angle of attack along the span for streamwise sections, resulting in a reduction of the over-all lift of the wing.

The reduction of the local angle of attack along the span of a sweptback wing also results in a destabilizing effect. This effect is indicated in figure 15(a) by the 3 percent \bar{c} forward shift of the aerodynamic center for configuration W_{w60}^{FT-6} and in figure 15(b) by the $4\frac{1}{2}$ percent forward shift in aerodynamic center for configuration W_{w60}^F . The preceding values of aerodynamic-center shift are averages taken over a range of lift coefficients from 0 to 0.4.

CONCLUSIONS

The results of an investigation to determine interaction effects between the wing and fuselage of a $\frac{1}{30}$ -scale semispan model of the Bell X-5 airplane at a Mach number of 1.24 are as follows:

1. The proportion of total lift carried over on the fuselage was about equal to the ratio of areas between the fuselage-wing intersection to the total wing area.

2. Wing interference on the fuselage tended to give a stabilizing effect, particularly at small angles of attack, which, at least partially, offset the destabilizing contribution of the isolated fuselage.

3. The lateral center of pressure location for the exposed wing panel moved outboard of the pivot point from 43 percent span of the exposed wing for 40° sweepback to 50 percent of the exposed wing for 60° sweepback.

4. The effect of increasing the flexibility of the 60° wing in bending by about $2\frac{1}{2}$ times was to reduce the lift-curve slope about 3 percent and to move the aerodynamic center forward about 4 percent of the mean aerodynamic chord.

Langley Aeronautical Laboratory
National Advisory Committee for Aeronautics
Langley Field, Va.

REFERENCES

1. Silsby, Norman S., Morris, Garland J., and Kennedy, Robert M.:
Longitudinal Characteristics at Mach Number of 1.24 of $\frac{1}{30}$ -Scale
Semispan Model of Bell X-5 Variable-Sweep Airplane with Wing Swept
Back 60° from Tests by NACA Wing-Flow Method. NACA RM L50E02a, 1950.
2. Morris, Garland J., Kennedy, Robert M., and Silsby, Norman S.: The
Effect of Sweepback on the Longitudinal Characteristics at a Mach
Number of 1.24 of a $\frac{1}{30}$ -Scale Semispan Model of the Bell X-5 Airplane
from Tests by the NACA Wing-Flow Method. NACA RM L50I28, 1950.
3. Sawyer, Richard H., Kennedy, Robert M., and Morris, Garland J.:
Longitudinal-Control Effectiveness and Downwash Characteristics at
a Mach Number of 1.24 of a $\frac{1}{30}$ -Scale Semispan Model of the
Bell X-5 Airplane As Determined by the NACA Wing-Flow Method. NACA
RM L50K15, 1951.
4. Kennedy, Robert M.: Effects of a Fuselage Flap Dive Brake on the
Aerodynamic Characteristics of $\frac{1}{30}$ -Scale Semispan Model of the
Bell X-5 Variable-Sweep Airplane at a Mach Number 1.24 As Deter-
mined by the NACA Wing-Flow Method. NACA RM L50L11a, 1951.
5. Johnson, Harold I.: Measurements of Aerodynamic Characteristics of
a 35° Sweptback NACA 65-009 Airfoil Model with $\frac{1}{4}$ -Chord Plain Flap
by the NACA Wing-Flow Method. NACA RM L7F13, 1947.

TABLE I

GEOMETRIC CHARACTERISTICS OF $\frac{1}{30}$ -SCALE SEMISPAN MODEL

OF BELL X-5 VARIABLE-SWEEP AIRPLANE

Wing dimensions:

Section (perpendicular to unswept 38.58 percent line of wing)			
Root		NACA 64(10)A011	
Tip		NACA 64(08)A008.6	
Sweepback angle	40°	50°	60°
Semispan, in.	5.31	4.60	3.88
Mean aerodynamic chord, in.	3.10	3.20	3.64
Chord at tip, in.	1.84	1.84	1.84
Chord at plane of symmetry, in.	4.40	4.50	4.25
Area (semispan), sq in.	14.97	14.20	13.79
Exposed area, sq in.	11.55	10.83	10.52
Aspect ratio	3.77	2.98	2.18
Dihedral (chord plane), deg	0	0	0
Incidence (chord plane), deg	0	0	0

Horizontal tail:

Section		NACA 64A006	
Semispan, in.			1.91
Mean aerodynamic chord, in.			1.43
Chord at tip, in.			0.72
Chord at plane of symmetry, in.			1.95
Area (semispan) sq in.			2.55
Aspect ratio			2.86
Height (above wing chord), in.			0.56
Length 0.26c of 60° swept wing to 0.25c _t , in.			6.83


 NACA

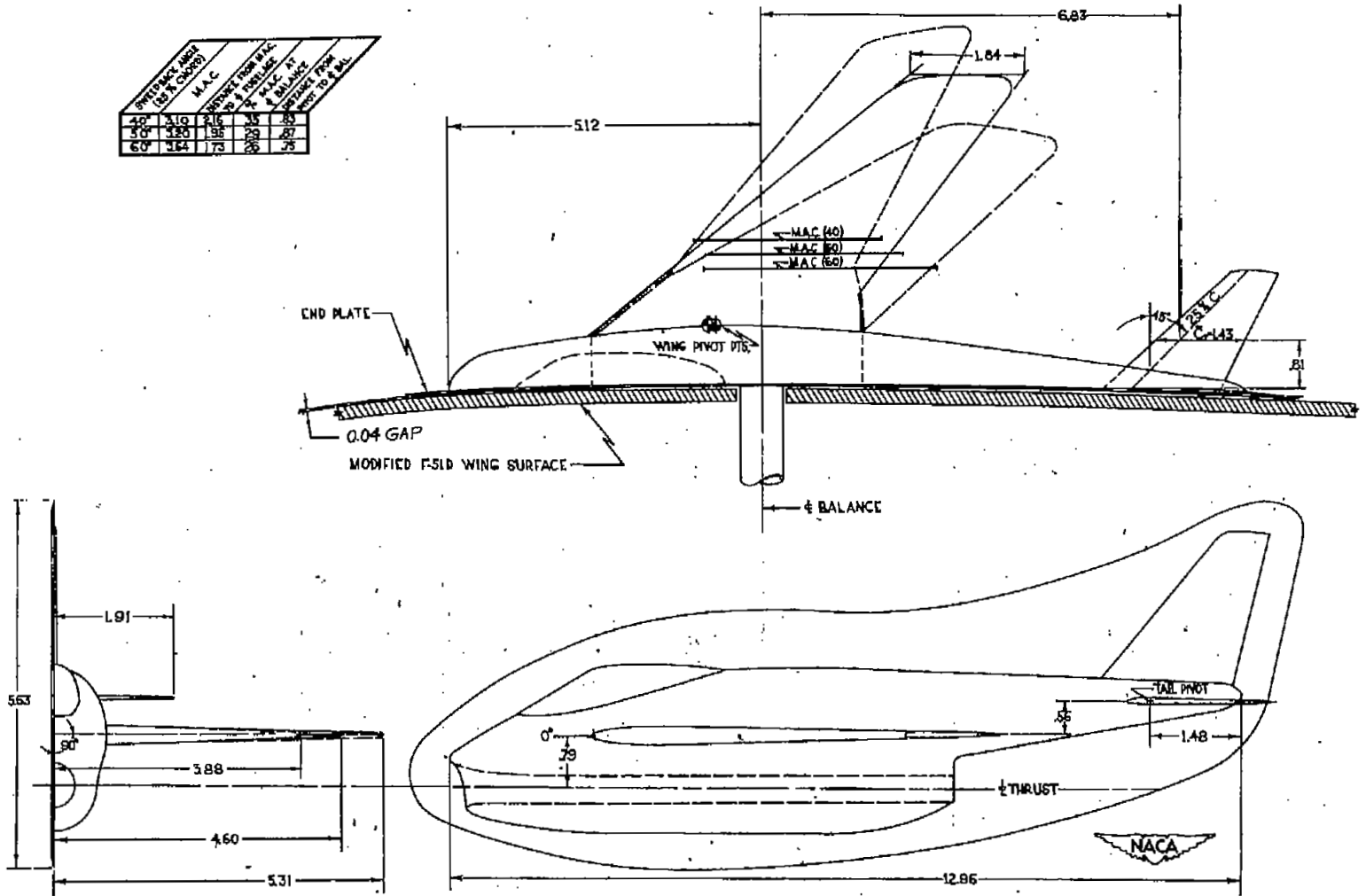


Figure 1.- Details of the semispan model of the Bell X-5 airplane with wing in 40°, 50°, and 60° sweep position. (All dimensions are in inches.)

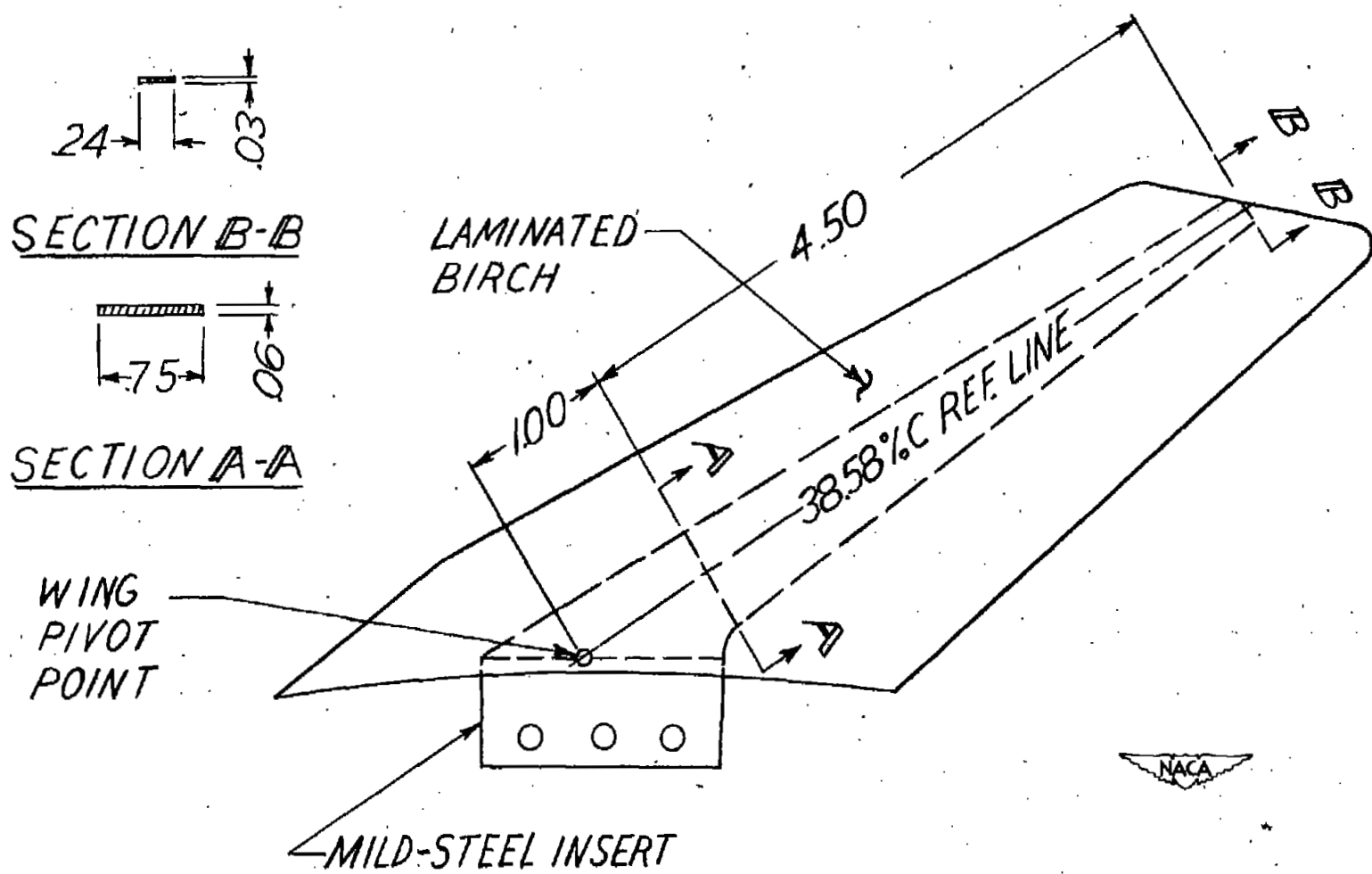


Figure 2.- Details of wooden wing. All dimensions are in inches.



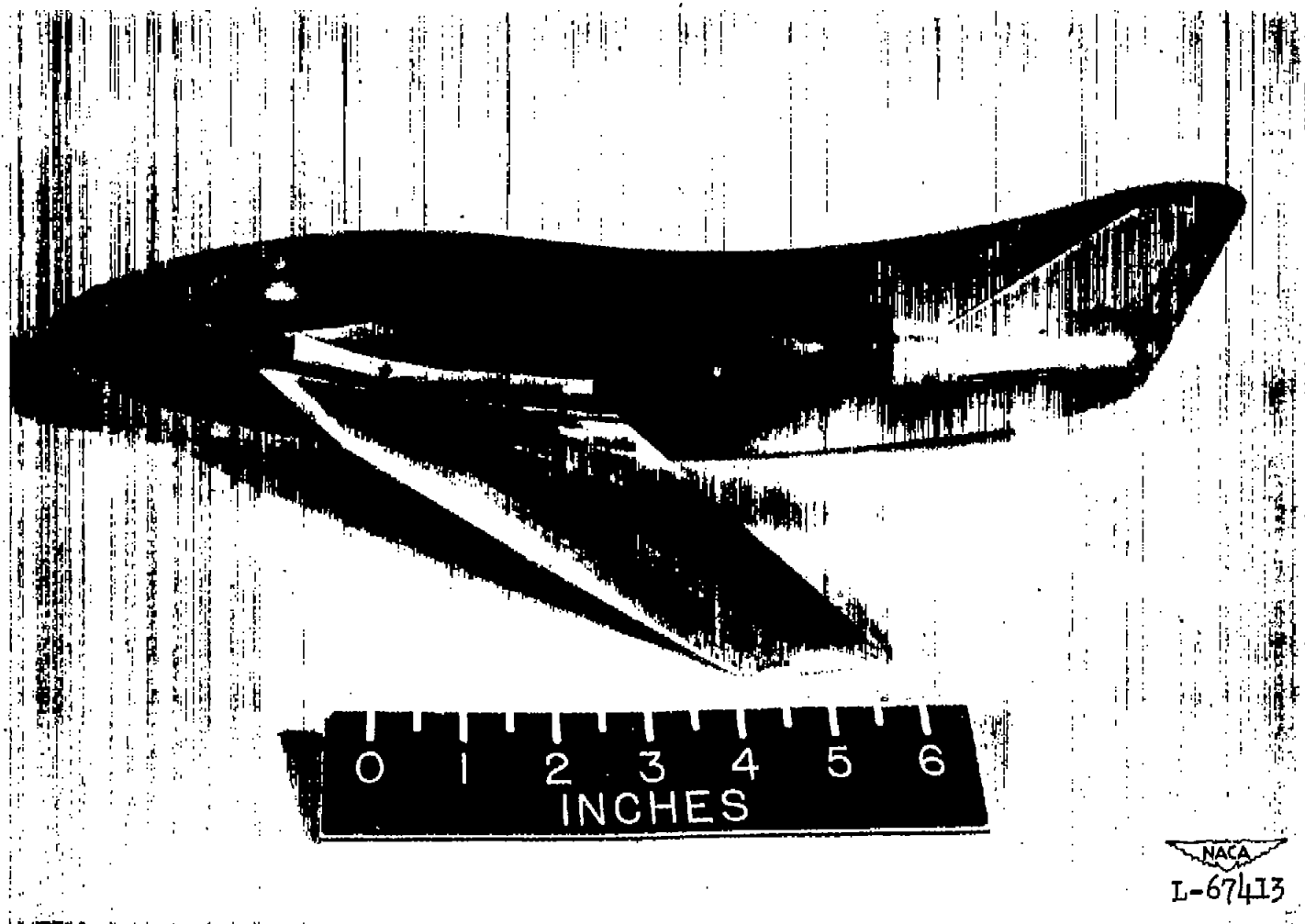


Figure 4.- Photograph of 60° sweptback wing with wing-root end plate attached, in presence of but detached from fuselage of Bell X-5 wing-flow model.

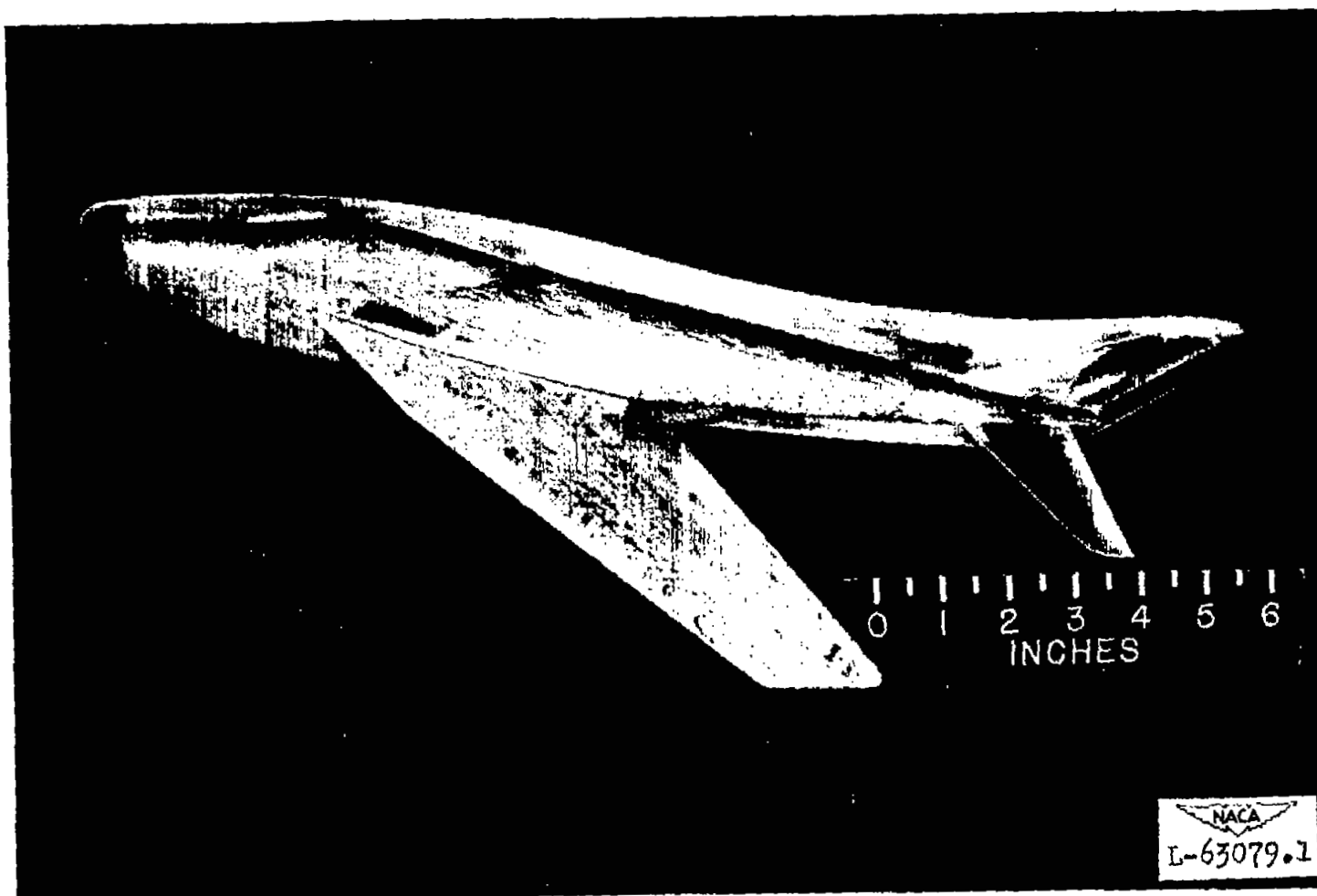


Figure 5.- Photograph of Bell X-5 semispan wing-flow model with 60° swept-back wood wing; $i_t = -6^\circ$.

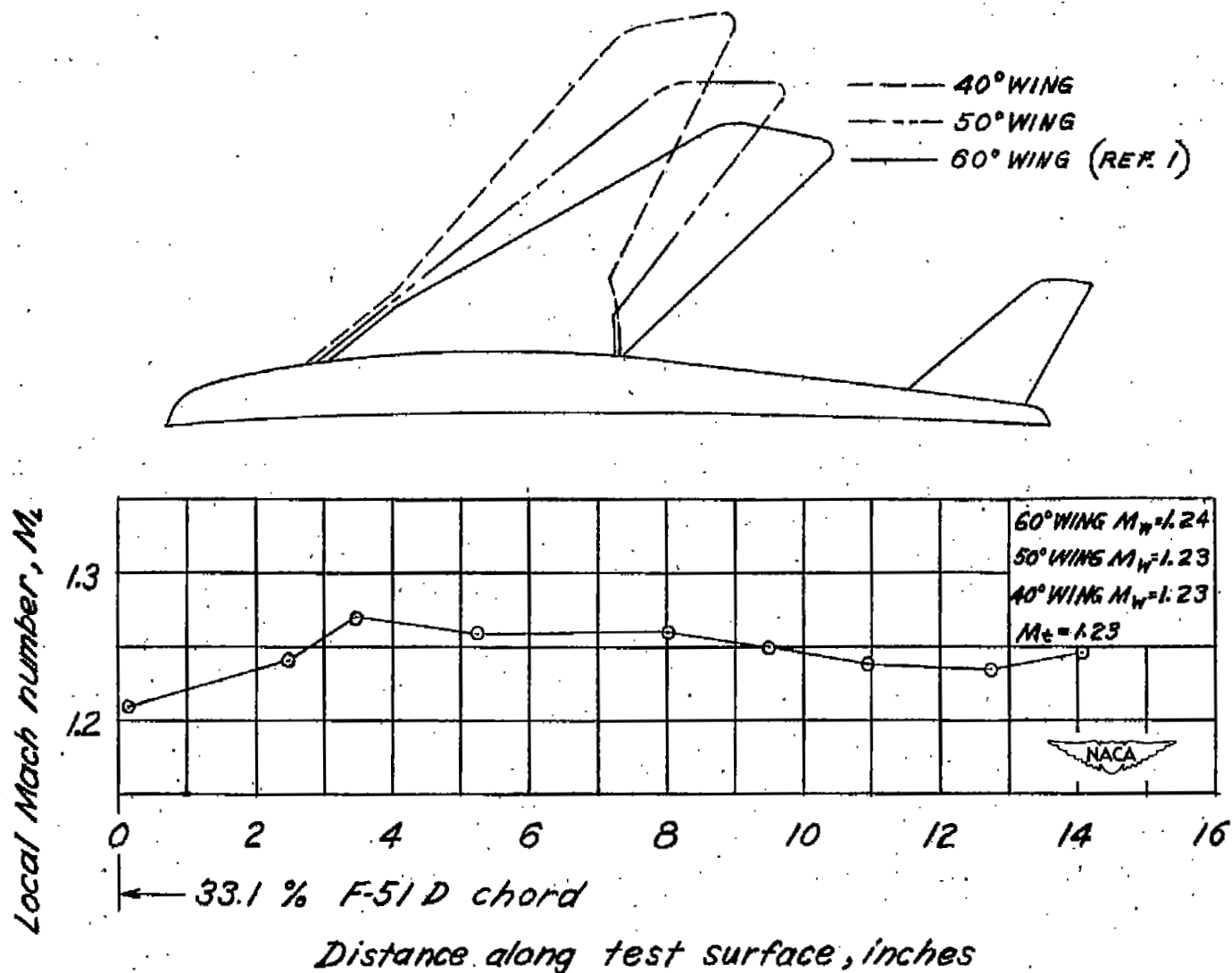
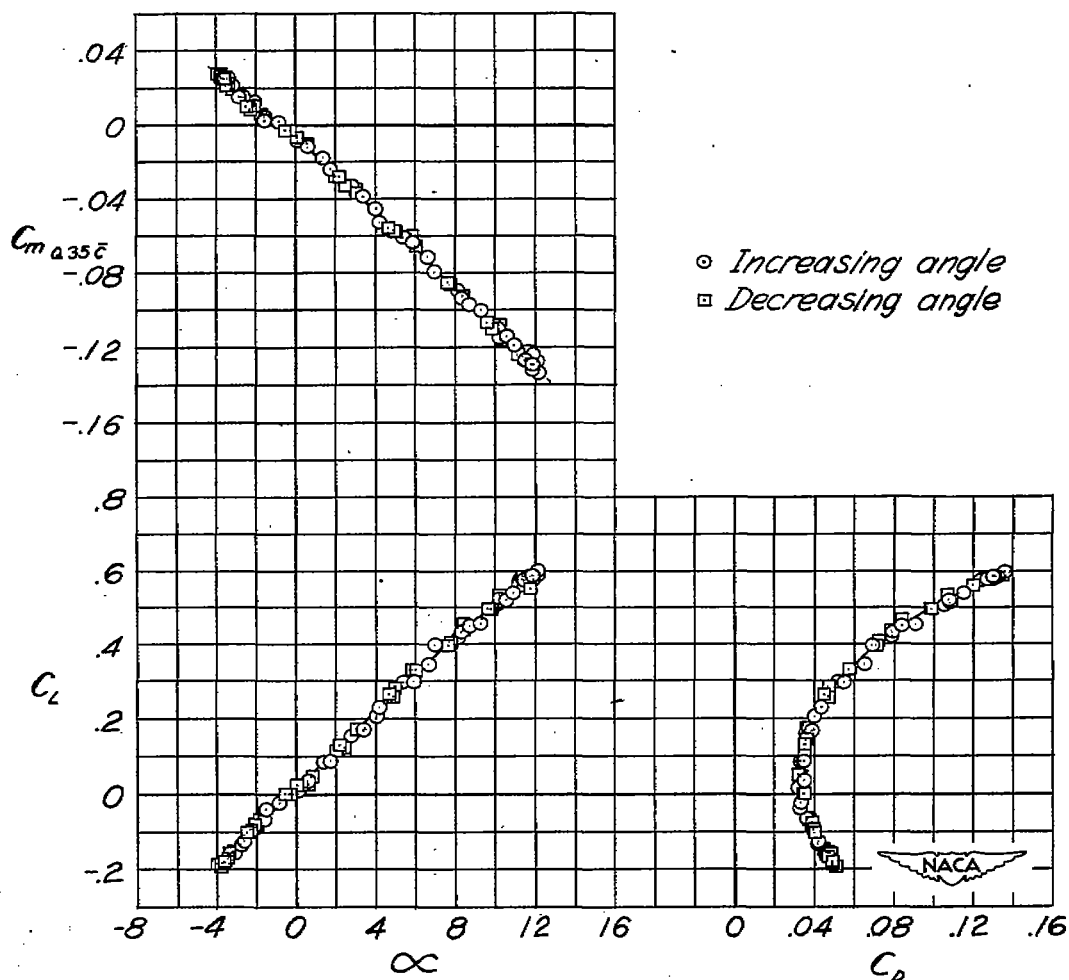
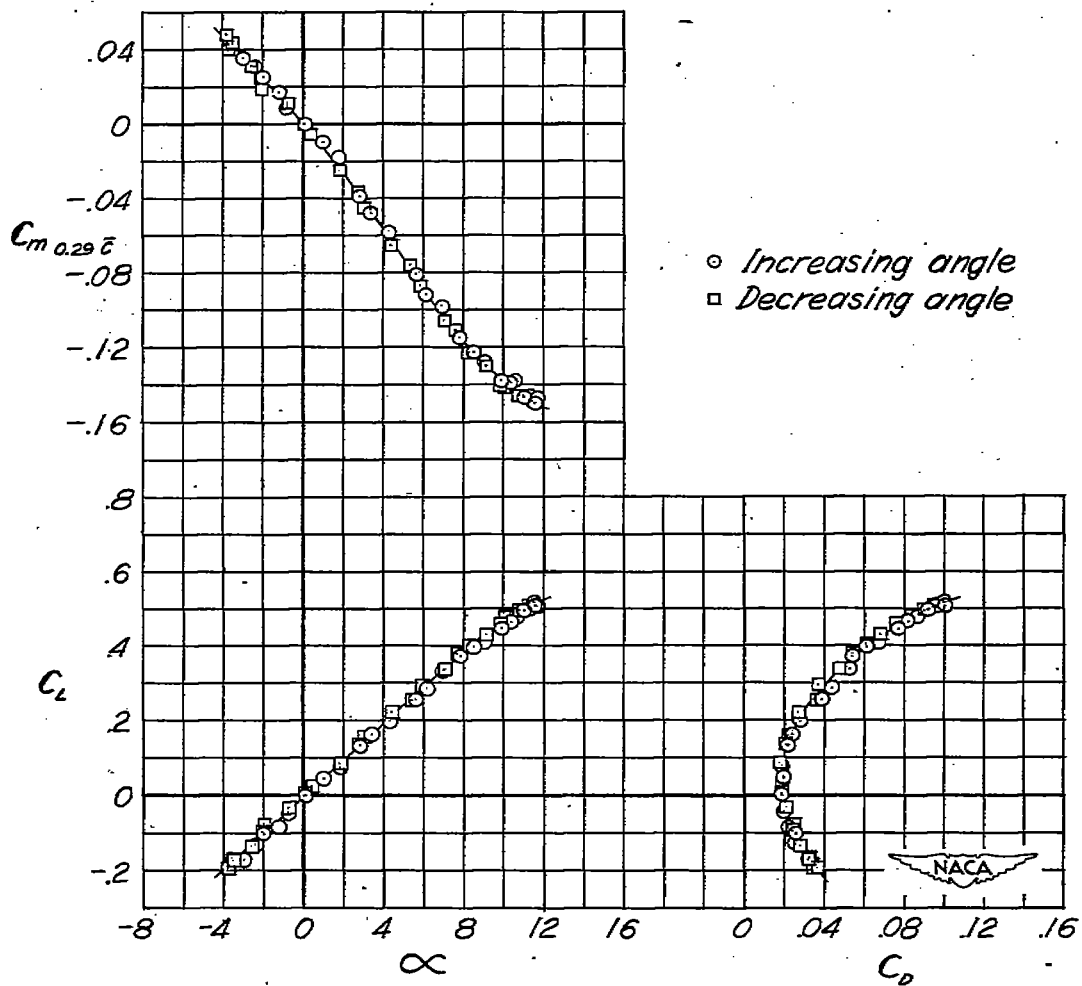


Figure 6.- Typical chordwise distribution of Mach number along the surface of test section. Chordwise location of model also shown.



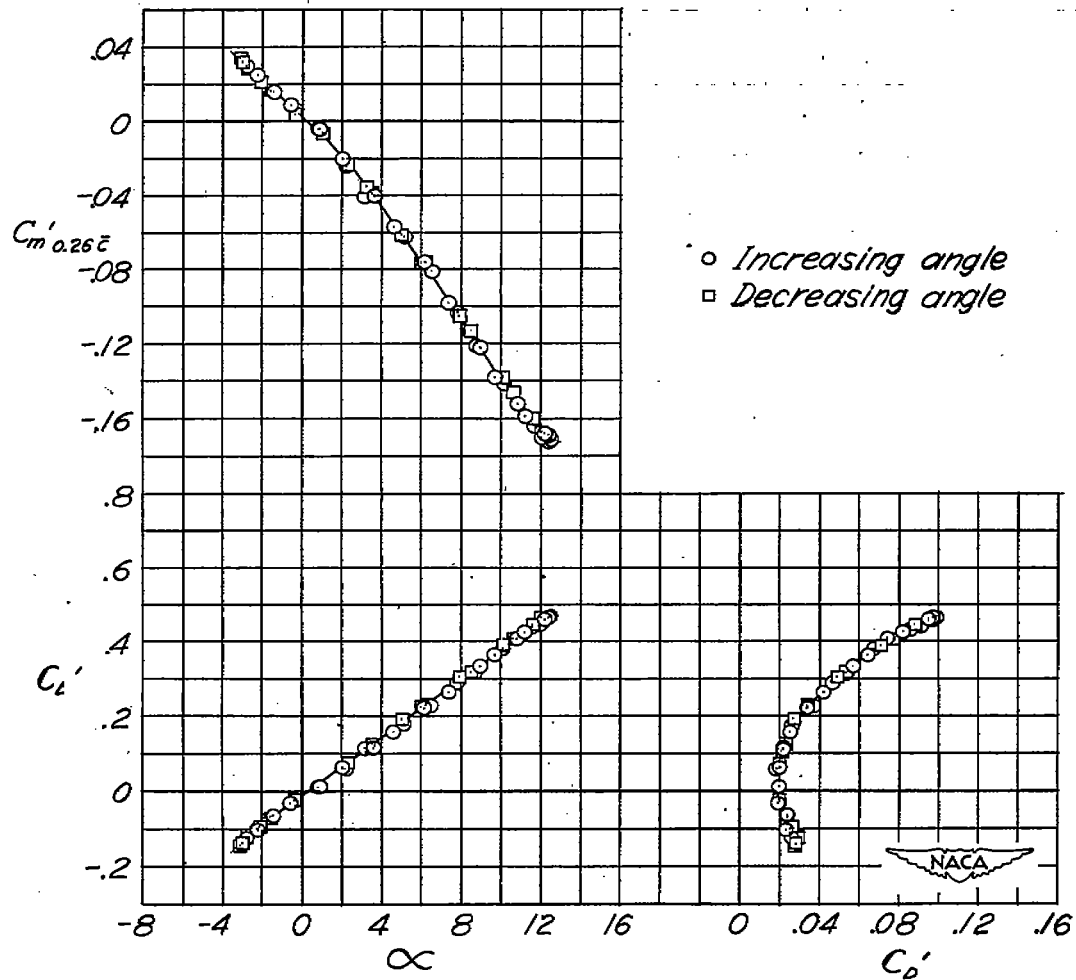
(a) $\Lambda = 40^\circ$ ($W_{40\alpha}^{F_{eg}}$).

Figure 7.- Aerodynamic characteristics of wing of semispan wing-flow model of Bell X-5 airplane in presence of but detached from model fuselage ($W_{\Lambda\alpha}^{F_{eg}}$); tail off; $M_W = 1.24$. (Coefficients based on respective wing dimensions.)



(b) $\Lambda = 50^\circ$ ($W_{50d}^F eg$).

Figure 7.- Continued.



(c) $\Lambda = 60^\circ$ ($W_{60d}^F eg$).

Figure 7.- Concluded.

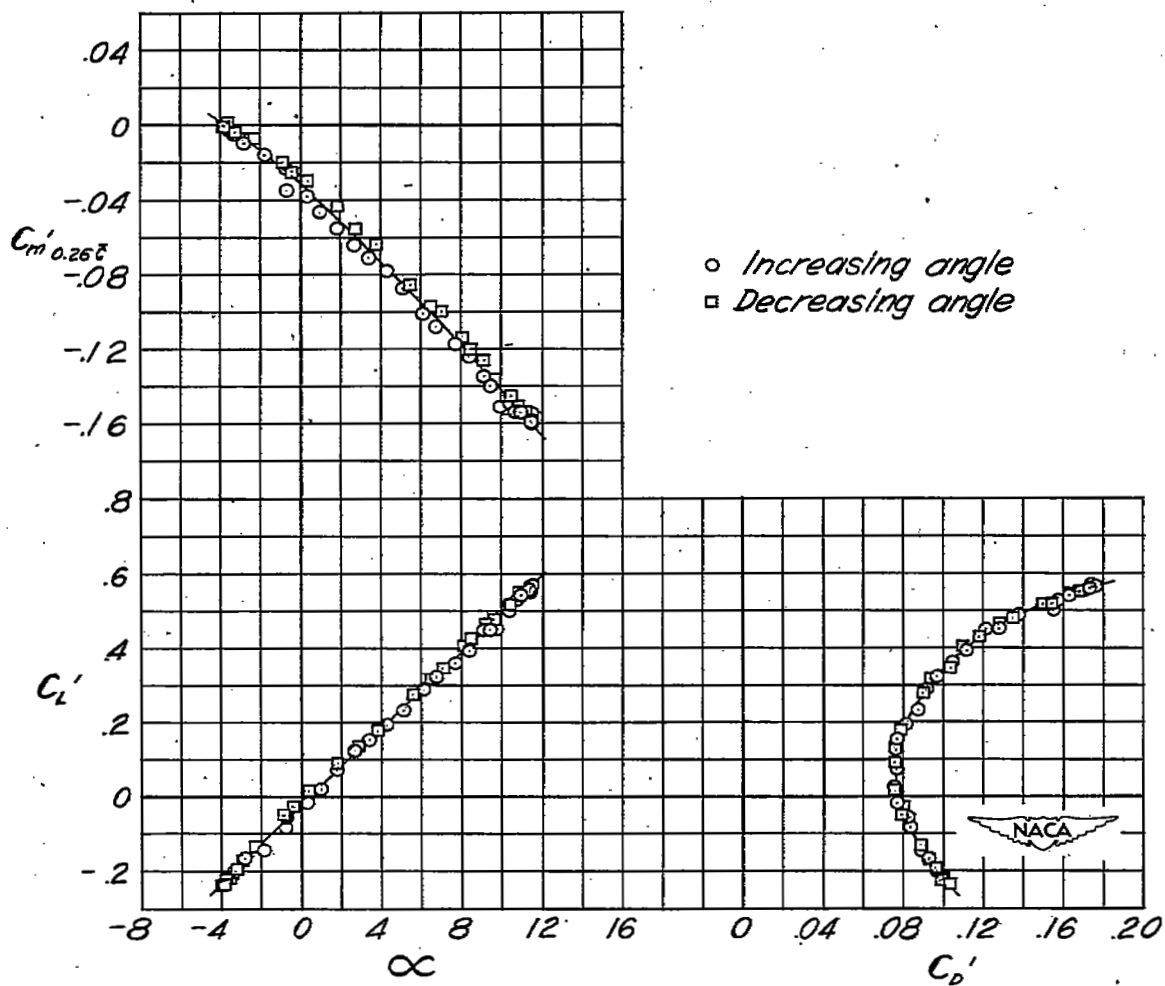


Figure 8.- Aerodynamic characteristics of semispan wing-flow model of Bell X-5 airplane with 60° wing and end plate and gap of configurations W_{Ad}^{Feg} simulated (W_{60}^{Feg}); tail off; $M_W = 1.24$. (Coefficients based on 60° wing dimensions.)

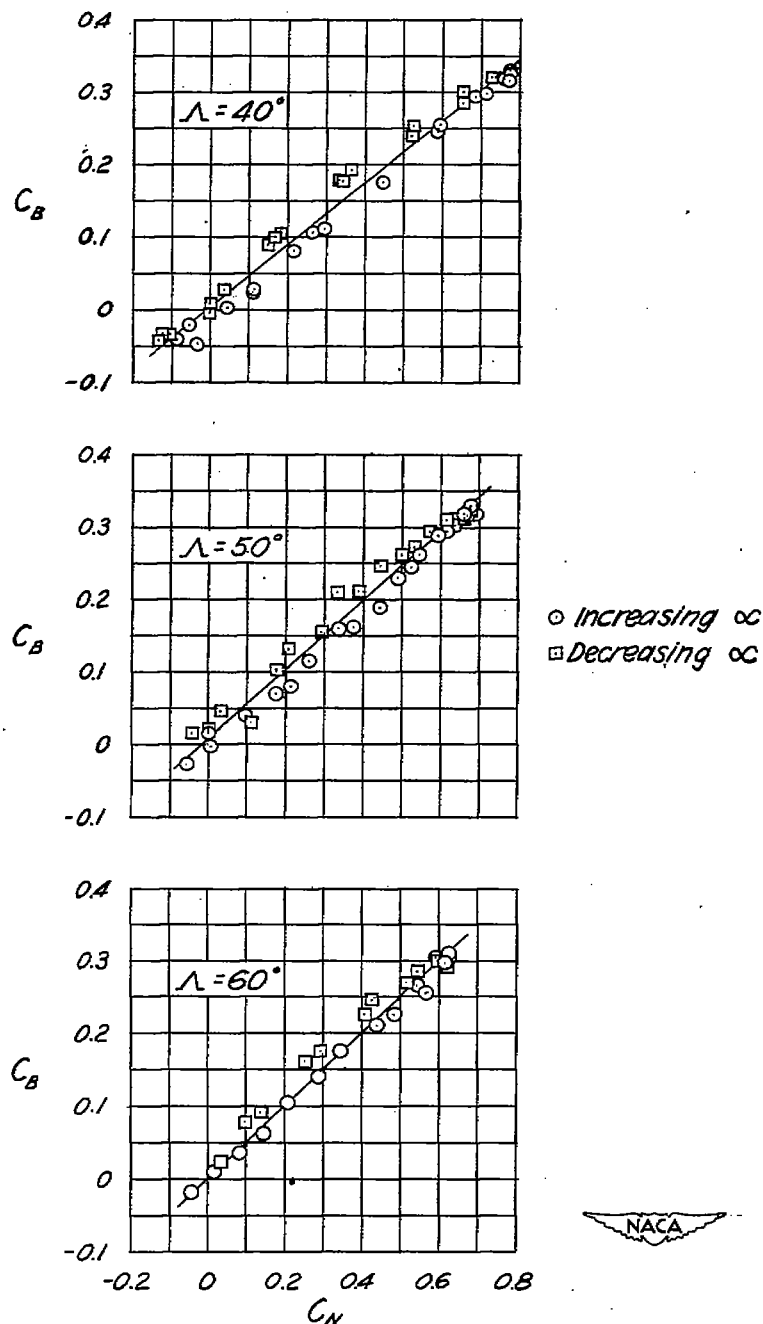


Figure 9.- Variation of bending-moment coefficient referred to the wing pivot point with normal-force coefficient of 40° , 50° , and 60° wings detached from fuselage of Bell X-5 semispan wing-flow model (W_{Ad}^{Feg}); tail off; $M_W = 1.24$. (Coefficients based on respective exposed-wing dimensions.)

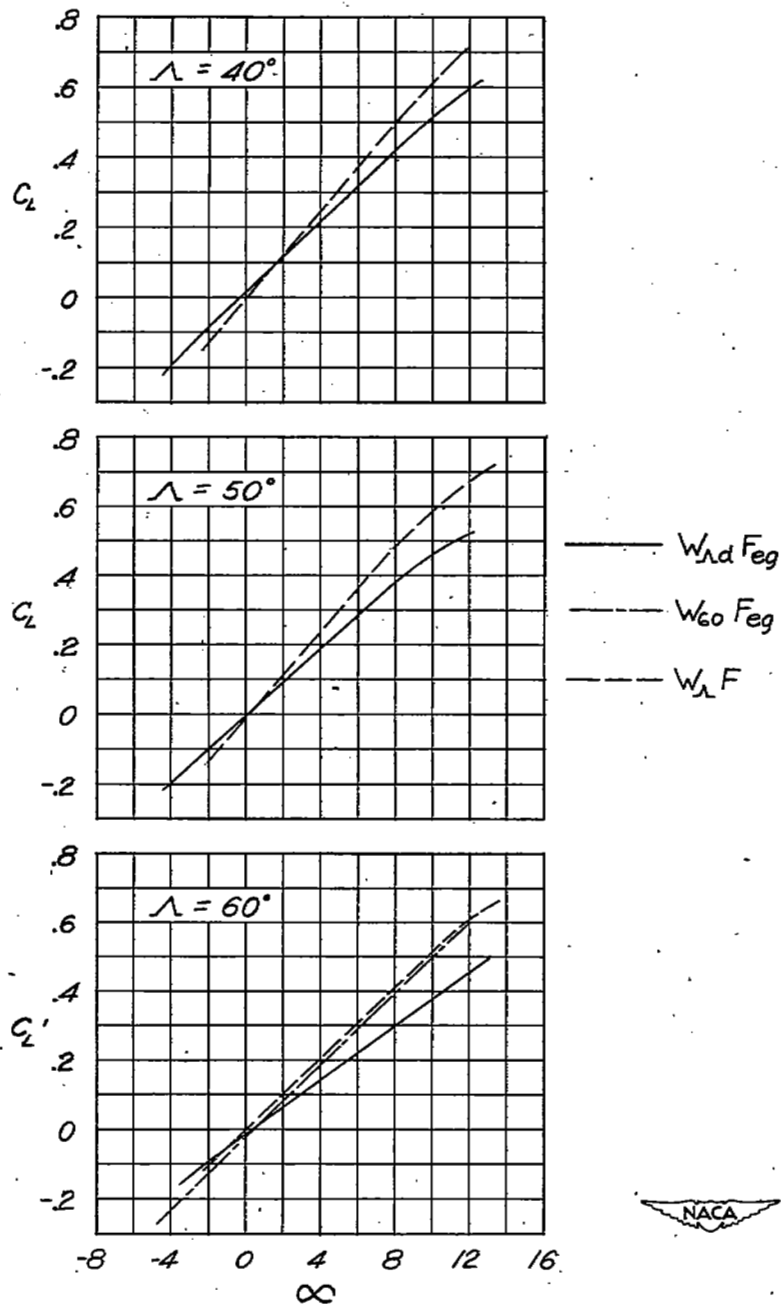


Figure 10.- Comparison of C_L against α curves of wing-detached configurations ($W_{\Lambda d} F_{eg}$) and the wing-fuselage configurations ($W_{\Lambda} F$) of reference 3. Configuration $W_{60} F_{eg}$ also shown. Bell X-5 semispan wing-flow model; tail off; $M_W = 1.24$. (Coefficients based on respective wing areas.)

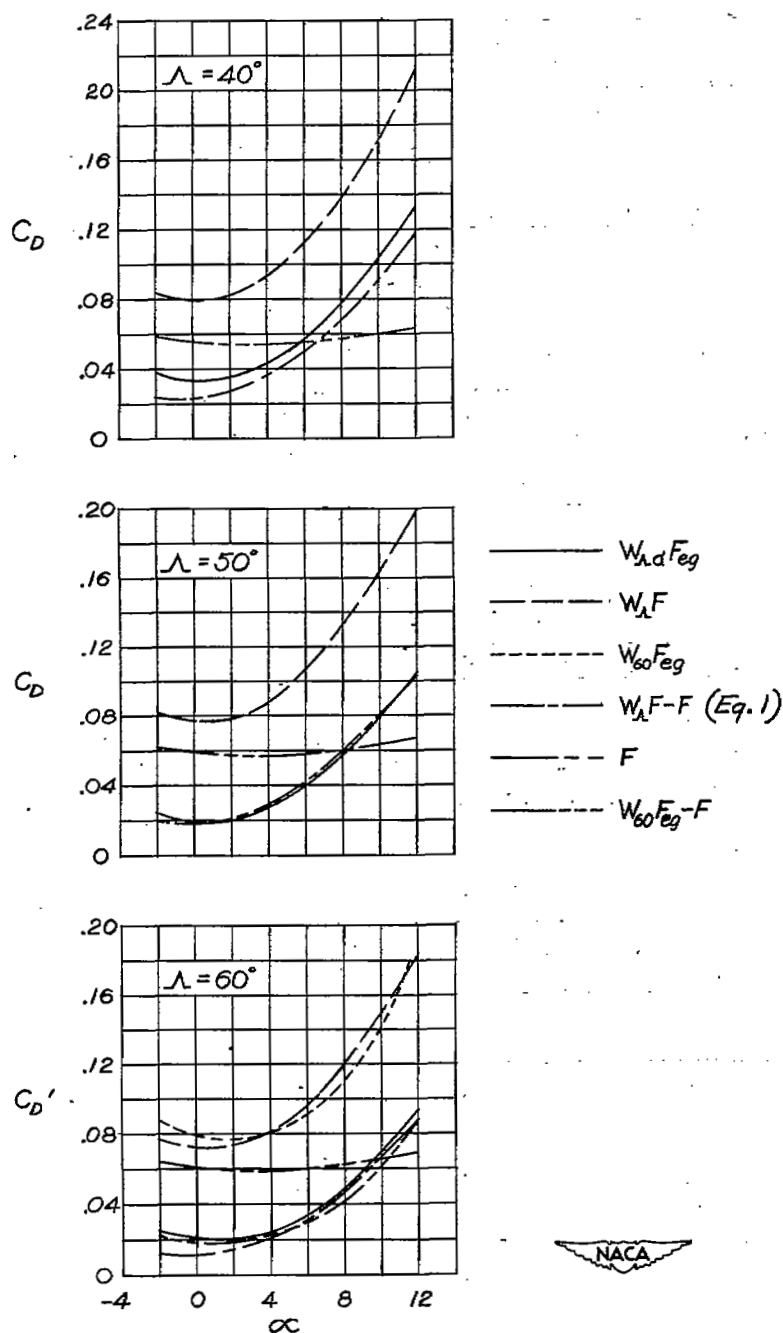


Figure 11.- Variation of C_D with α for the three sweepback angles tested for various configurations. Bell X-5 semispan wing-flow model; tail off; $M_W = 1.24$. (Coefficients based on respective wing areas.)

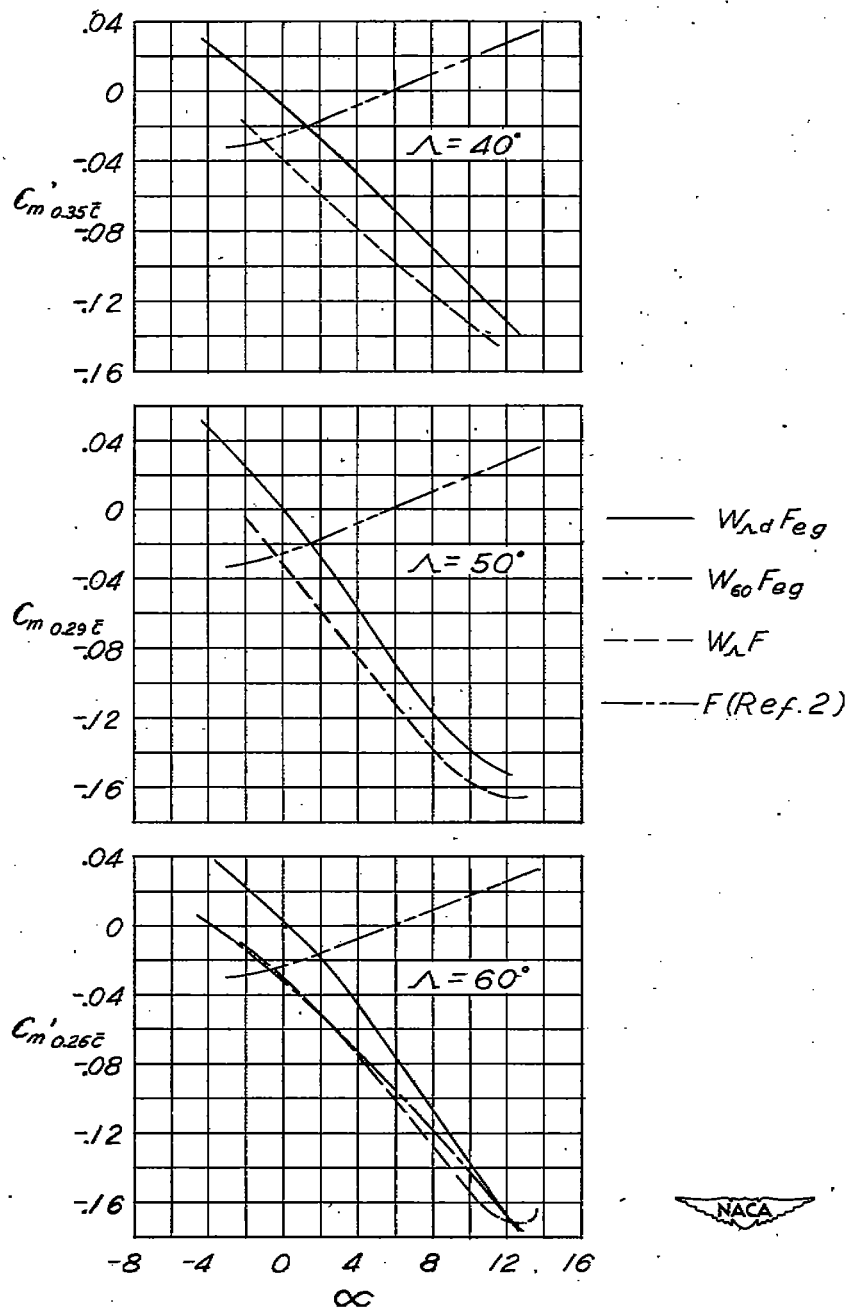


Figure 12.- Comparison of C_m against α curves of wing-detached configurations ($W_{\Lambda d} F_{eg}$) and the wing-fuselage configurations ($W_{\Lambda} F$) of reference 3. Configurations $W_{60} F_{eg}$ and F also shown. Bell X-5 semispan wing-flow model; tail off; $M_w = 1.24$. (Coefficients based on dimensions of respective wings.)

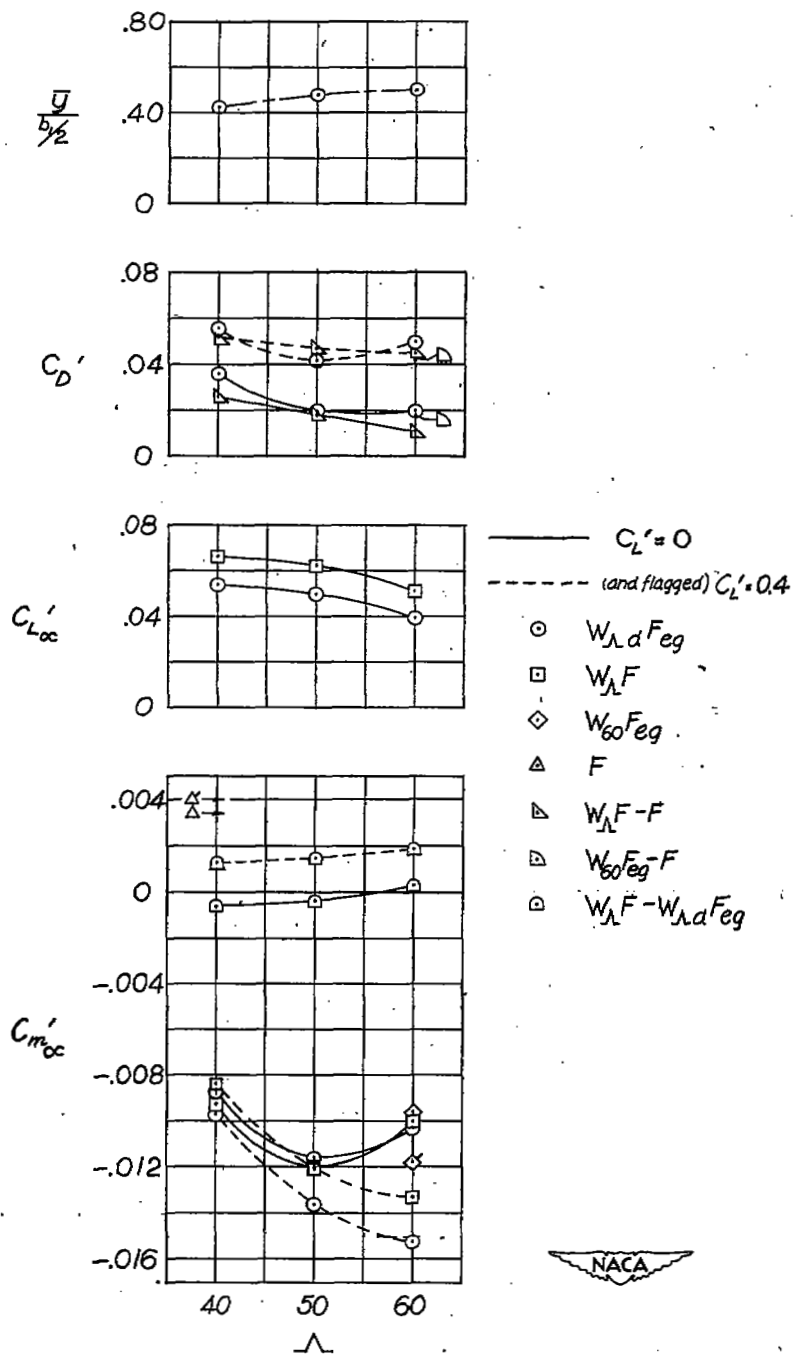
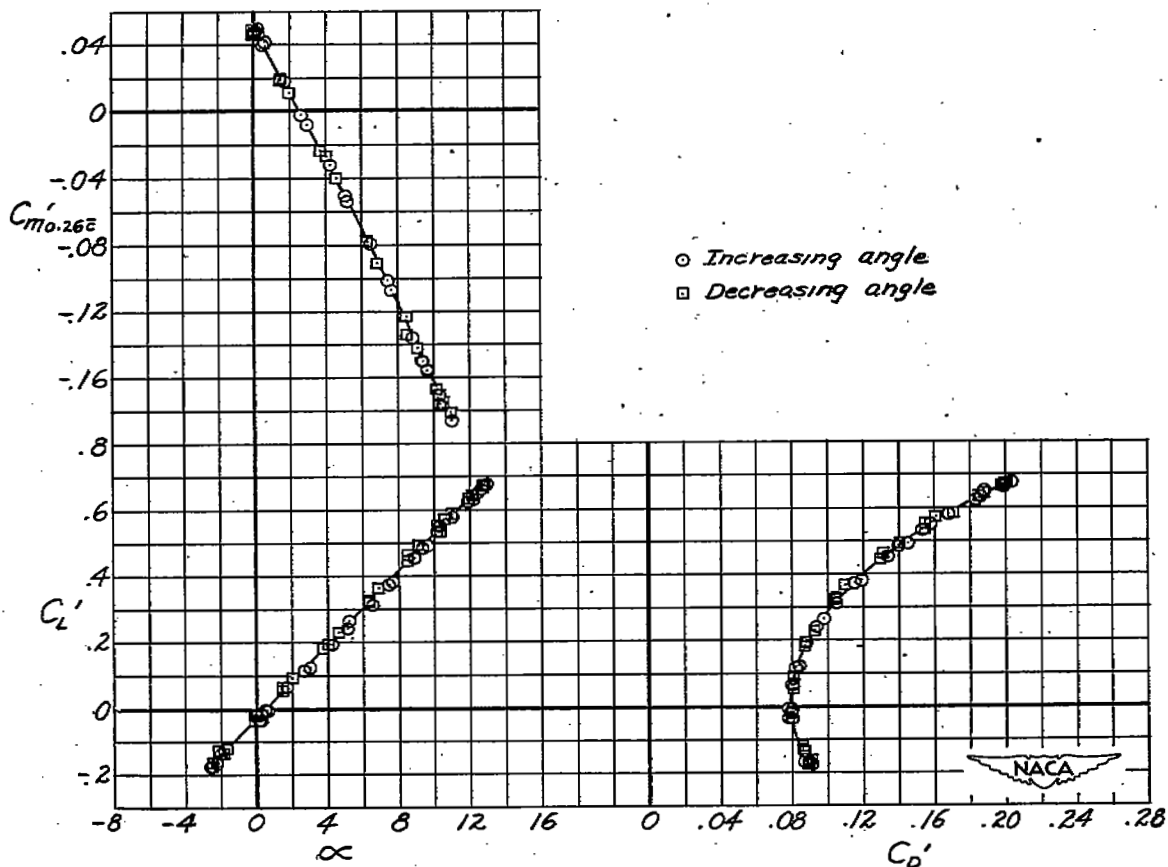
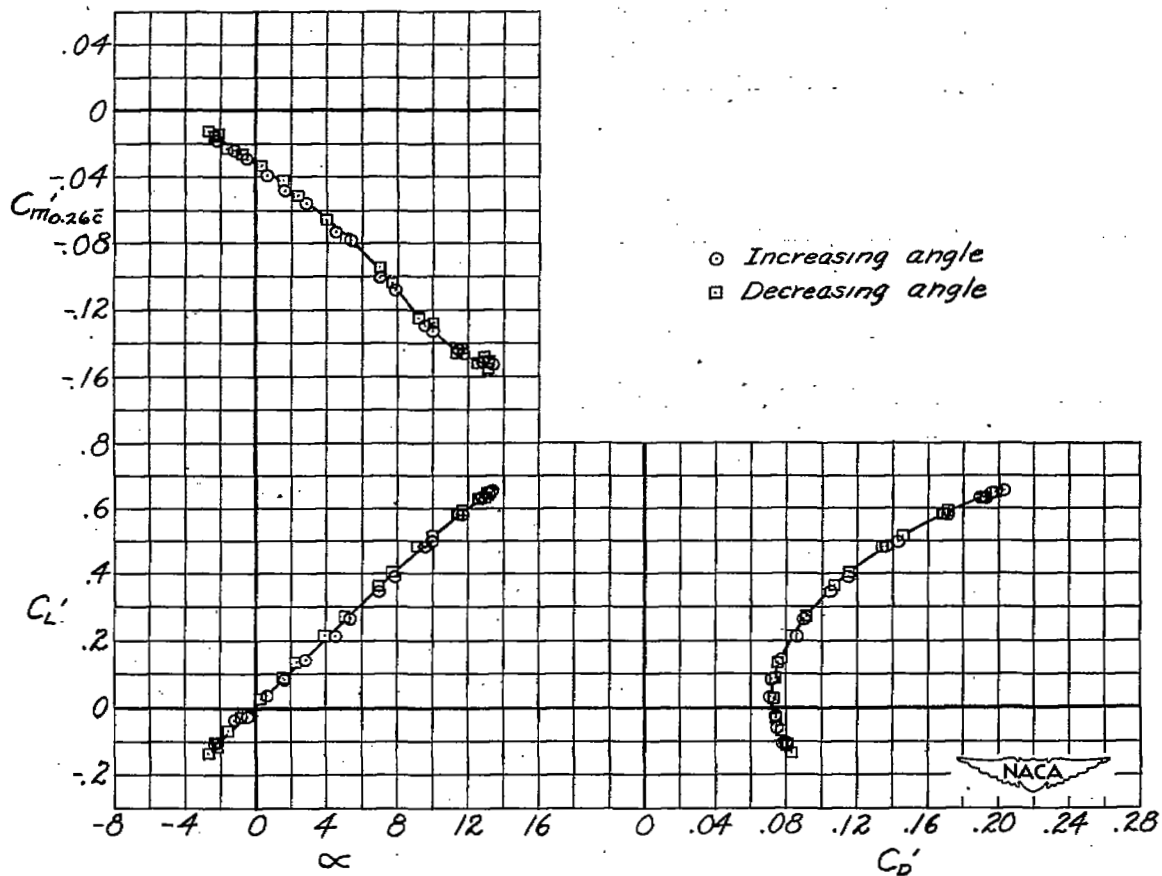


Figure 13.- Effect of sweepback angle on spanwise center-of-pressure location, and on drag coefficient, slope of lift curve, and stability parameter $C_{m'\alpha}$ at $C_L' = 0$ and $C_L' = 0.4$ for various configurations. Bell X-5 semispan wing-flow model; tail off; $M_W = 1.24$. (Coefficients based on dimensions of 60° wing.)



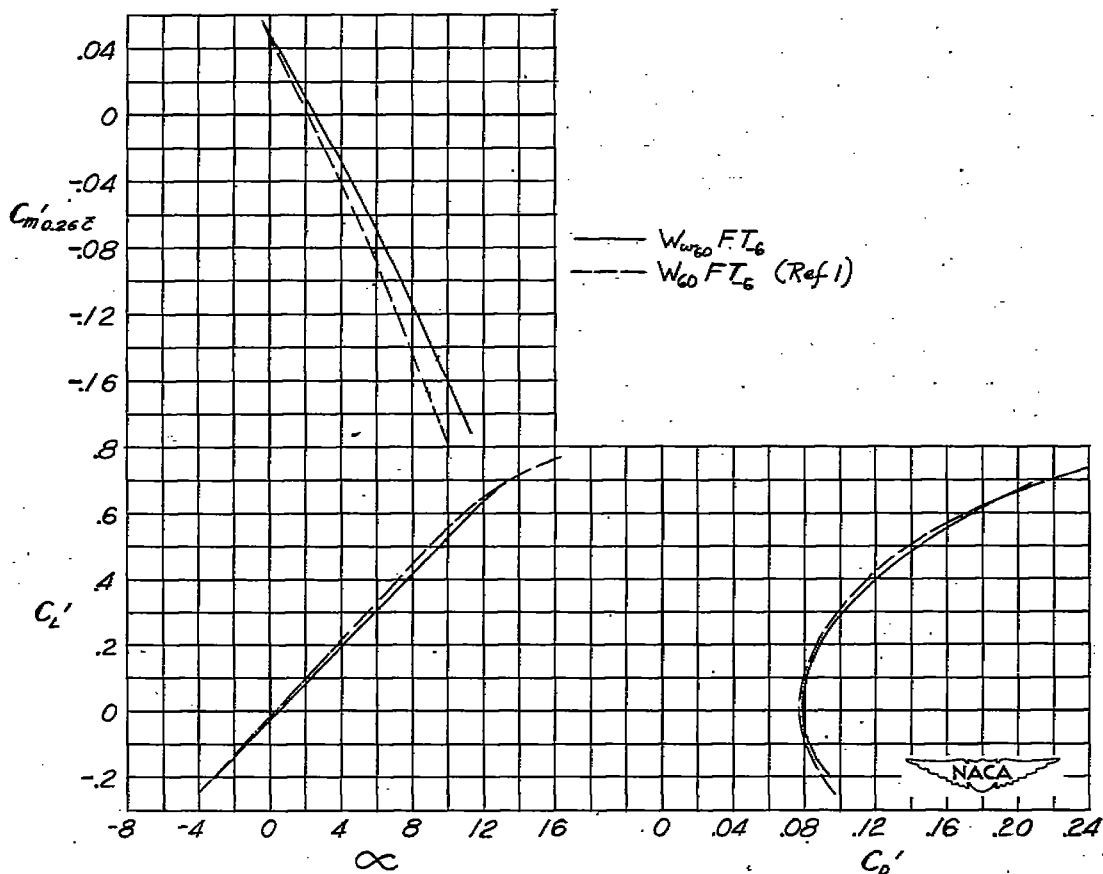
(a) With tail ($W_w 60^{FT-6}$).

Figure 14.- Aerodynamic characteristics of semispan wing-flow model of Bell X-5 airplane equipped with a wooden wing. $\Lambda = 60^\circ$, $M_w = 1.24$.
(Coefficients based on dimensions of 60° wing.)



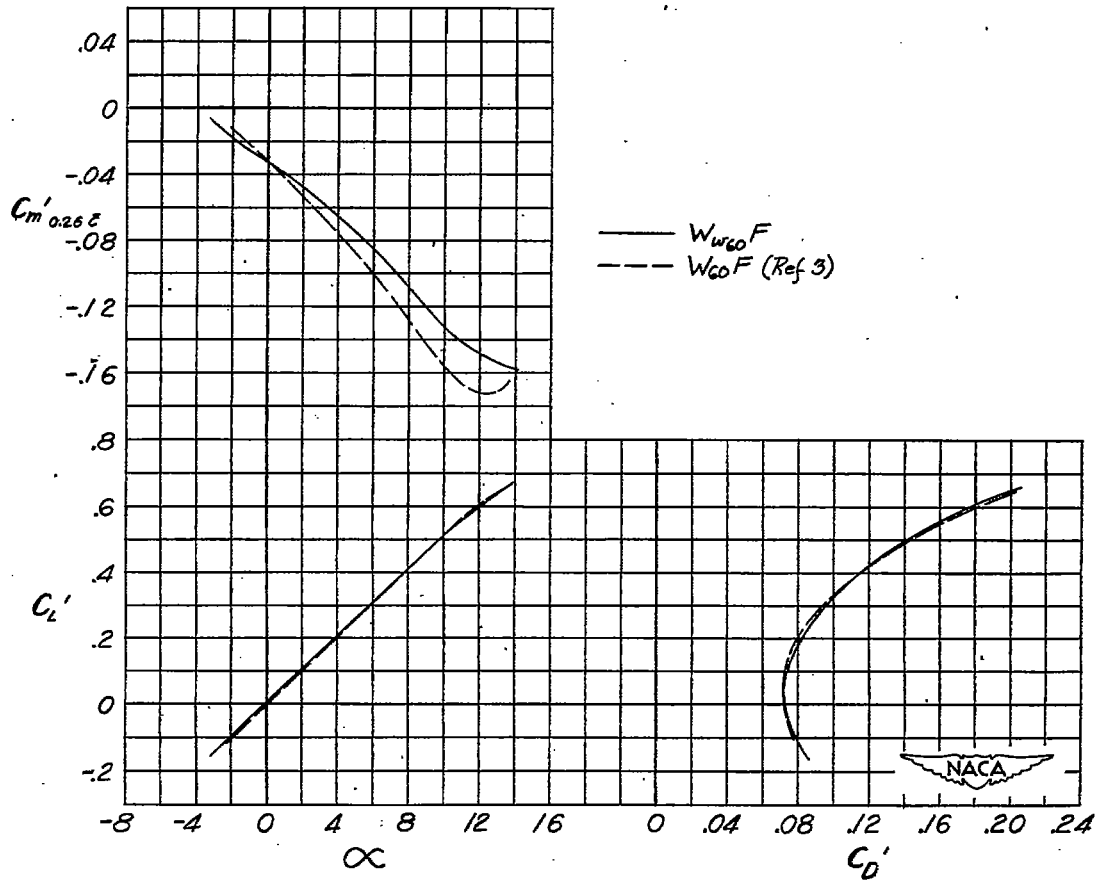
(b) Tail off (W_{W60F}).

Figure 14.- Concluded.



(a) Tail on.

Figure 15.- Comparison of aerodynamic characteristics of semispan model of Bell X-5 airplane equipped with a wooden wing with those of the model equipped with a dural wing. $\Lambda = 60^\circ$, $M_W = 1.24$. (Coefficients based on dimensions of 60° wing.)



(b) Tail off.

Figure 15.- Concluded.

SECURITY INFORMATION

NASA Technical Library



3 1176 01436 9038

